

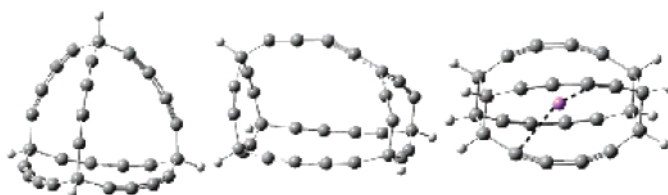
## Computational Studies of Ethynyl- and Diethynyl-Expanded Tetrahedranes, Prismanes, Cubanes, and Adamantanes

Steven M. Bachrach\* and Dustin W. Demoin

Department of Chemistry, Trinity University, 1 Trinity Place, San Antonio, Texas 78212

sbachrach@trinity.edu

Received February 6, 2006



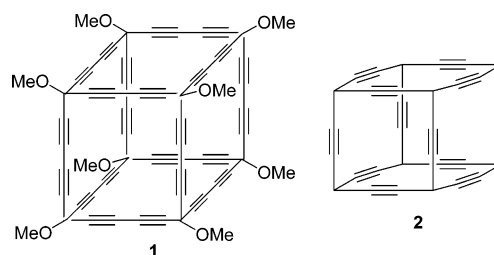
B3LYP/6-31+G(d) and MP2/6-31+G(d) computations were performed on a series of ethynyl- and diethynyl-expanded tetrahedranes, prismanes, cubanes and adamantanes. Every ethynyl expansion reduces the ring strain energy of the cage. The deprotonation energies of the cage poly-yne are exceptionally low; we estimate that the gas-phase deprotonation energy of the diethynyl-expanded cubane is about 309 kcal mol<sup>-1</sup>. The ring and cage poly-yne can serve as effective hosts of either lithium or sodium cation, where the best host maximizes the number of interactions of alkynyl groups with the cation at an ideal distance. Last, the vertical excitation energies of the poly-yne and their conjugate bases suggest that the alkynyl groups are interacting through space. The poly-yne express a broad range of absorption energies, indicating that these molecules are potential targets in expressly designed optical applications.

### Introduction

Since the discovery of acetylenic coupling in 1869,<sup>1</sup> implementation of adjoining sp-hybridized carbon atoms has been of broad interest. In recent years, interest has piqued in two applications of poly-yne. The first application is the possibility of creating one-, two-, and three-dimensional macrocycles that have rigid scaffolding for use in molecular recognition,<sup>2</sup> and the second is their use as molecular switches and in electro-optical devices.<sup>3–5</sup>

The research group of Diederich has been the leader in constructing novel buta-1,3-diyne-expanded molecules. Their recent synthesis<sup>6</sup> of the diethynyl-expanded cubane **1** is especially notable, as it is the first example of the potential for building of conjugated  $\pi$ -systems in three-dimensions.

We reported a computational study of the singly expanded cubane analogue **2**. In particular, we noted its reduced ring strain



energy (relative to cubane), its ability to act as a cation acceptor and its especially low deprotonation energy ( $\Delta G_{\text{DPE}} = 325$  kcal mol<sup>-1</sup>).<sup>7</sup> Diederich and Houk examined the diethynyl-expanded cubane and tetrahedrane, noting the reduced strain of these expanded compounds, and developed a force field for predicting the structures of very large ethynyl-expanded structures.<sup>8</sup>

This study continues upon our previous work by examining a range of three-dimensional shapes incorporating the ethynyl or diethynyl linker. We examine the 3-D poly-yne **4** and **5** derived from tetrahedrane **3**, the poly-yne **7–14** derived from prismane **6**, the poly-yne **16–18** derived from cubane **15**, and the poly-yne **20** derived from adamantane **19** (Chart 1). A variety

(1) Glaser, C. *Ber. Dtsch. Chem. Ges.* **1869**, *2*, 422–424.

(2) Siemsen, P.; Livingston, R. C.; Diederich, F. *Angew. Chem., Int. Ed.* **2000**, *39*, 2632–2657.

(3) Gobbi, L.; Seiler, P.; Diederich, F. *Angew. Chem., Int. Ed. Engl.* **1999**, *38*, 674–678.

(4) Diederich, F. *Chem. Commun.* **2001**, 219–227.

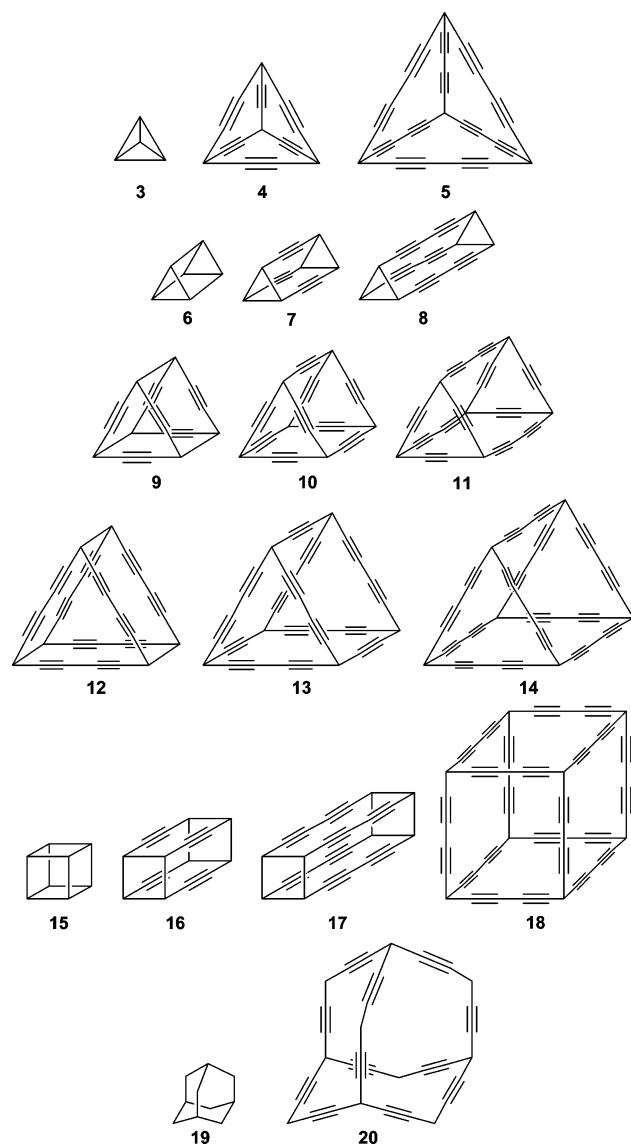
(5) Nielsen, M. B.; Diederich, F. *Chem. Record* **2002**, *2*.

(6) Manini, P.; Amrein, W.; Gramlich, V.; Diederich, F. *Angew. Chem., Int. Ed.* **2002**, *41*, 4339–4343.

(7) Bachrach, S. M. *J. Phys. Chem. A* **2003**, *107*, 4957–4961.

(8) Jarowski, P. D.; Diederich, F.; Houk, K. N. *J. Org. Chem.* **2005**, *70*, 1671–1678.

CHART 1



of different properties are computed and compared: their structures, ring strain energies (RSE), and cation affinities. Potential application of extended  $\pi$ -conjugation in multiple dimensions as electrooptical devices depends on their optical properties. Toward that end, we have determined the vertical excitation energy for these conjugated molecules and their anions and show that these molecules can be tuned for a particular frequency and that conjugation can extend into three different directions.

### Computational Methods

All structures were completely optimized within the appropriate point group. Since deprotonation energies (DPE) are to be computed, the 6-31+G(d) basis set was employed in order to adequately describe the anions.<sup>9–12</sup> All structures were optimized using the B3LYP<sup>13</sup> method. Since B3LYP can provide poor

DPEs,<sup>11,12</sup> MP2/6-31+G(d) optimizations were performed for many of the compounds. MP2 DPEs are generally in excellent agreement with experiments.<sup>10</sup> Unfortunately, MP2 computation of many of the larger molecules are beyond our computational resources, so a means for extrapolating the B3LYP results to fit the MP2 data was explored and is detailed below. Compounds for which extrapolated values are used are explicitly noted in the tables below.

The nature of all structures was ascertained with analytical frequencies, which are used without scaling to compute 298 K thermal contributions to enthalpies and free energies using standard partition-function approximations.<sup>14</sup> Again, the size of the molecules posed computational limitations, so frequencies were computed for only a few species at MP2 and for all of them (except **18** and its conjugate base **18cb**) at B3LYP. Calculation of the vertical excitation energies was carried out using the TDDFT<sup>15–17</sup> method with the B3LYP functional and the 6-31+G(d) basis set with the B3LYP/6-31+G(d) optimized geometry. All computations were performed using GAUSSIAN-03.<sup>18</sup>

### Results and Discussion

**Structure and Ring Strain Energy (RSE).** To assess the structures of the 3-D expanded polyynes, we first discuss the structures of the simple acyclic alkynes (**21–23**) and the cyclic alkynes (**25, 26, 28–33**) (Chart 2), which represent the faces of the  $\pi$ -expanded molecules. Their critical geometric parameters ( $C_{sp} \equiv C_{sp}$ ,  $C_{sp^3} - C_{sp}$ , and  $C_{sp} - C_{sp}$  distances and  $C_{sp^3} - C_{sp} \equiv C_{sp}$  and  $C_{sp} \equiv C_{sp} - C_{sp}$  angles) computed at both B3LYP/6-31+G(d) and MP2/6-31+G(d) are listed in Table S1 (in the Supporting Information). The two different computational levels produce very similar structures, with the  $C_{sp} \equiv C_{sp}$  bond slightly longer and the  $C_{sp} \equiv C_{sp} - C_{sp}$  angle slightly larger at MP2 than at B3LYP. The  $C_{sp} \equiv C_{sp}$  distance is about 1.22 Å and does not change appreciably when embedded into the ring systems. The angle about the  $C_{sp}$  atom is ideally 180°, and it is very close to that value in the acyclic alkynes. The angle is bent substantially away from linearity in most of the cyclic poly-ynes. This results from the interplay of increasing the angle at the saturated carbon, thereby relieving its strain, at the expense of bending about the sp carbon and inducing angle strain at that atom. This can be seen

(13) (a) Becke, A. D. *J. Chem. Phys.* **1993**, *98*, 5648–5650. (b) Lee, C.; Yang, W.; Parr, R. G. *Phys. Rev. B* **1988**, *37*, 785–789. (c) Vosko, S. H.; Wilk, L.; Nusair, M. *Can. J. Phys.* **1980**, *58*, 1200–1211. (d) Stephens, P. J.; Devlin, F. J.; Chabalowski, C. F.; Frisch, M. J. *J. Phys. Chem.* **1994**, *98*, 11623–11627.

(14) Cramer, C. J. *Essentials of Computational Chemistry. Theories and Models*; John Wiley: Chichester, UK, 2002.

(15) Petersilka, M.; Gossman, U. J.; Gross, E. K. U. *Phys. Rev. Lett.* **1996**, *76*, 1212–1215.

(16) Casida, M. E.; Jamorski, C.; Casida, K. C.; Salahub, D. R. *J. Chem. Phys.* **1998**, *108*, 4439–4449.

(17) Stratmann, R. E.; Scuseria, G. E.; Frisch, M. J. *J. Chem. Phys.* **1998**, *109*, 8218–8224.

(18) Frisch, M. J.; Trucks, G. W.; Schlegel, H. B.; Scuseria, G. E.; Robb, M. A.; Cheeseman, J. R.; Montgomery, J., J. A.; Vreven, T.; Kudin, K. N.; Burant, J. C.; Millam, J. M.; Iyengar, S. S.; Tomasi, J.; Barone, V.; Mennucci, B.; Cossi, M.; Scalmani, G.; Rega, N.; Petersson, G. A.; Nakatsuji, H.; Hada, M.; Ehara, M.; Toyota, K.; Fukuda, K.; Hasegawa, J.; Ishida, M.; Nakajima, T.; Honda, Y.; Kitao, O.; Nakai, H.; Klene, M.; Li, X.; Knox, J. E.; Hratchian, H. P.; Cross, J. B.; Adamo, C.; Jaramillo, J.; Gomperts, R.; Stratmann, R. E.; Yazyev, O.; Austin, A. J.; Cammi, R.; Pomelli, C.; Ochterski, J. W.; Ayala, P. Y.; Morokuma, K.; Voth, G. A.; Salvador, J.; Dannenberg, J. J.; Zakrzewski, V. G.; Dapprich, S.; Daniels, A. D.; Strain, M. C.; Farkas, O.; Malick, D. K.; Rabuck, A. D.; Raghavachari, K.; Foresman, J. B.; Ortiz, J. V.; Cui, Q.; Baboul, A. G.; Clifford, S.; Cioslowski, J.; Stefanov, B. B.; Liu, G.; Liashenko, A.; Piskorz, P.; Komaromi, I.; Martin, R. L.; Fox, D. J.; Keith, T.; Al-Laham, M. A.; C. Y. Peng, C. Y.; Nanayakkara, A.; Challacombe, M.; Gill, P. M. W.; Johnson, B.; Chen, W.; Wong, M. W.; Gonzalez, C.; Pople, J. A. *GAUSSIAN-03*; Gaussian, Inc.: Pittsburgh, PA, 2003.

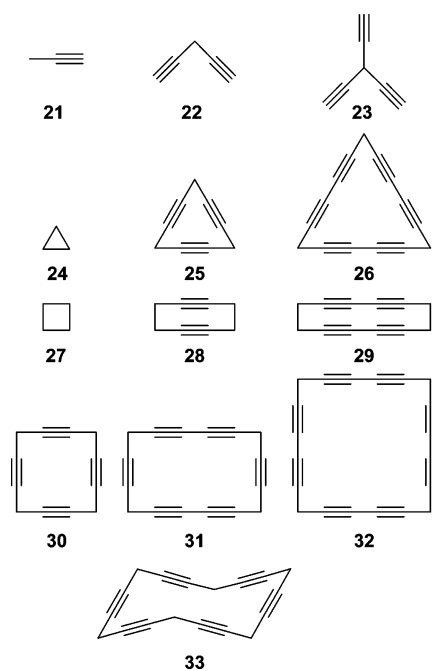
(9) Chandrasekhar, J.; Andrade, J. G.; Schleyer, P. v. R. *J. Am. Chem. Soc.* **1981**, *103*, 5609–5612.

(10) Saunders Jr., W. H. *J. Phys. Org. Chem.* **1994**, *7*, 268–271.

(11) Merrill, G. N.; Kass, S. R. *J. Phys. Chem.* **1996**, *100*, 17465–17471.

(12) Burk, P.; Koppel, I. A.; Koppel, I.; Leito, I.; Travnikova, O. *Chem. Phys. Lett.* **2000**, *323*, 482–489.

CHART 2



seen in the increasing angle about the saturated carbon of  $60.0^\circ$ ,  $101.8^\circ$ , and  $106.9^\circ$  in **24**, **25**, and **26**, respectively, while the angle about the sp carbons is  $159.1^\circ$  in **25** and  $165.2^\circ$  in **26**.

The geometric parameters of the 3-D cage poly-yne (listed in Table S1) are similar to those of their monocyclic analogues. The structures are also presented in Figure 1. The  $C_{sp}\equiv C_{sp}$  distance is about  $1.22 \text{ \AA}$ , except for **4**, **5**, **7**, and **8**, where MP2 predicts it to be about  $1.24 \text{ \AA}$ . The  $C_{sp^3}-C_{sp}$  bonds are also generally slightly longer in the 3-D poly-yne. The angles about the  $C_{sp}$  atom increase as the size of the ring increases. In summary, the distances and angles in the 3-D poly-yne are really quite similar to those in their monocyclic analogues.

The expanded prismanes **9** and **12** structures computed at B3LYP are unusual. The  $C_{sp^3}-C_{sp^3}$  distances are exceptionally long:  $1.706 \text{ \AA}$  in **9** and  $1.694 \text{ \AA}$  in **12**. In both of these prismanes, the two triangular faces are each strained, with the  $\pi$ -bonds bowing out to relieve the angle strain at the saturated carbon. Forcing these two faces to be close to each other, connected by a C–C single bond, induces an additional strain from the interfacial  $\pi$ -bond repulsion. Since the single-configuration DFT method is unlikely to adequately describe these stretched C–C bonds—one might conceive of these two prismanes as interacting pairs of triradical faces—we will leave further analysis and discussion of these species for a separate paper.

Since the variation in angles is reflective of strain energy, we evaluated the ring strain enthalpy (RSE) of the monocyclic and 3-D poly-yne using the group equivalent method.<sup>19</sup> The group equivalent method is a homodesmotic reaction that also preserves the number and type of groups as defined by Benson.<sup>20</sup> The ring strain enthalpy is then the negative of the reaction enthalpy. This approach is used to assess the ring strain energy of a wide variety of strained molecules.<sup>21</sup> The group equivalent reactions for representative poly-yne are shown in Scheme 1.

(19) Bachrach, S. M. *J. Chem. Educ.* **1990**, *67*, 907–908.

(20) Benson, S. W. *Thermochemical Kinetics*; 2nd ed.; Wiley-Interscience: New York, 1976.

The calculated RSE at B3LYP and MP2 are listed in Table 1. Given the size of many of the compounds, we were unable to compute the analytical frequencies, or even an optimized structure, for some compounds at MP2. For the largest molecule, **18**, we were unable to compute analytical frequencies at B3LYP/6-31+G(d). However, there is an excellent linear correlation ( $r^2 > 0.99$ ) between the RSE computed with just the electronic energies ( $\Delta E_{RSE}$ ) and those computed using the enthalpies ( $\Delta H_{RSE}^{298}$ ) for both the B3LYP and MP2 values. These estimated ring strain enthalpies based on the  $\Delta E_{RSE}$  are listed where appropriate in Table 1.

Examination of the B3LYP and MP2 RSEs reveals significant discrepancies. Notable is the very low estimate of the RSE of cubane at B3LYP ( $141.6 \text{ kcal mol}^{-1}$ ), while the MP2 estimate ( $167.4 \text{ kcal mol}^{-1}$ ) is in fine agreement with a previous estimate<sup>22</sup> of  $166 \text{ kcal mol}^{-1}$  or the value of  $164.8 \text{ kcal mol}^{-1}$  obtained using the group equivalent reaction and experimental<sup>23</sup> heats of formation. Disturbingly, the MP2 and B3LYP RSE values for the poly-yne differ by 3–15  $\text{kcal mol}^{-1}$ . The general success of MP2 to predict RSE calls into question the B3LYP values. Furthermore, the recent studies that note the gross failure of B3LYP to predict bond dissociation energies,<sup>24–26</sup> especially as molecules become systematically larger, cast doubt on the B3LYP RSE values.

Given our insufficient computational resources to handle all of the molecules with the MP2 method, we are forced to make use of the B3LYP results. (This need is even more pressing with the calculations of deprotonation energies and spectral properties discussed later.) We sought a multiple regression relation that could adequately fit the MP2 RSEs from the B3LYP values. A quite acceptable fit was found with eq 1 ( $r^2 = 0.998$ ),

$$\Delta H_{RSE}^{298}(\text{MP2, predicted}) = 0.883\Delta H_{RSE}^{298}(\text{B3LYP}) + 6.83N_{3MR} + 7.02N_{4MR} - 1.00N_{\text{trip}} - 0.078 \quad (1)$$

where  $N_{3MR}$  is the number of three-member rings,  $N_{4MR}$  is the number of four-member rings, and  $N_{\text{trip}}$  is the number of triple bonds in the molecule. The MP2-predicted RSEs that result from the application of eq 1 are listed in Table 2, and we will use these values or the actual MP2 RSEs in the discussion that follows.

For the monocyclic poly-yne, the RSE decreases with each insertion of an ethynyl group. Thus, the RSEs of **24**, **25**, and **26** are 27.1, 22.3, and  $5.4 \text{ kcal mol}^{-1}$ . This parallels the increase in the angles about the saturated and sp carbons. The same trend exists for the ethynyl-expansion of the four-member ring. In fact, the large poly-yne **31–33** are essentially strain-free. Each ethynyl insertion allows for the angles at the saturated carbons to relax toward their unstrained values.

This same trend occurs for the 3-D poly-yne. The RSEs of the tetrahydrides **3**, **4**, and **5**, decrease from 140.2 to  $77.6$  to

(21) (a) Novak, I. *J. Chem. Inf. Model.* **2004**, *44*, 903–906. (b) Bach, R. D.; Dmitrenko, O. *J. Am. Chem. Soc.* **2004**, *126*, 4444–4452. (c) Bissett, K. M.; Gilbert, T. M. *Organometallics* **2004**, *23*, 5048–5053. (d) Gilbert, T. M. *Organometallics* **2000**, *19*, 1160–1165. (e) Bachrach, S. M.; Gailbreath, B. D. *J. Am. Chem. Soc.* **1998**, *120*, 3528–3529. (f) Bachrach, S. M. *J. Phys. Chem.* **1993**, *97*, 4996–5000.

(22) Eaton, P. E. *Angew. Chem., Int. Ed. Engl.* **1992**, *31*, 1421–1436.

(23) Mallard, W. G.; Linstrom, P. J. *NIST Chemistry Webbook—June 2005 Release*; U.S. Secretary of Commerce: Washington, DC, 2005

(24) Check, C. E.; Gilbert, T. M. *J. Org. Chem.* **2005**, *70*, 9828–9834.

(25) Izgorodina, E. I.; Coote, M. L.; Radom, L. *J. Phys. Chem. A* **2005**, *109*, 7558–7566.

(26) Yao, X.-Q.; Hou, X.-J.; Jiao, H.; Xiang, H.-W.; Li, Y.-W. *J. Phys. Chem. A* **2003**, *107*, 9991–9996.

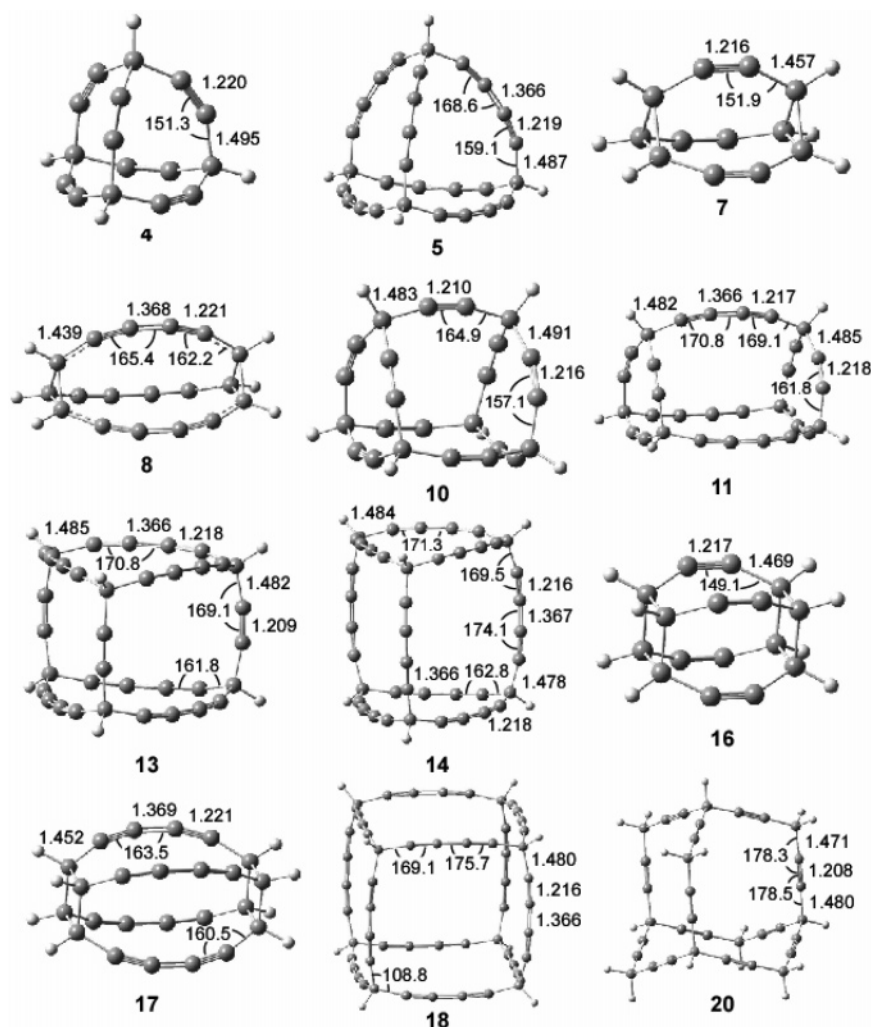
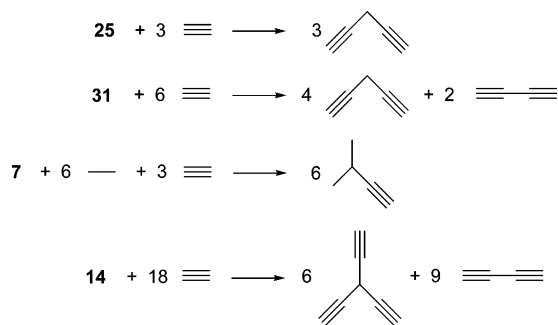


FIGURE 1. B3LYP/6-31+G(d) optimized geometries of the cage poly-yne. All distances are in angstroms and all angles are in degrees.

#### SCHEME 1



39.5 kcal mol<sup>-1</sup>, respectively. Each ethynyl insertion into the prismane reduces its RSE, so that the parent prismane **6** is quite strained (its RSE is 148.5 kcal mol<sup>-1</sup>), but the completely diethynyl-expanded prismane **14** is less strained than cyclopropane or cyclobutane; its RSE is only 22.1 kcal mol<sup>-1</sup>. Cubane is very strained, but insertion of four ethynyl groups, giving **16**, reduces the RSE by over 30 kcal mol<sup>-1</sup>, and insertion of four diethynyl groups (**17**) reduces the RSE by nearly 80 kcal mol<sup>-1</sup>. The cubane with ethynyl groups inserted into all 12 C–C bonds (**2**) has an exceptionally low RSE of 33.3 kcal mol<sup>-1</sup>. This is lower than our previous estimate,<sup>7</sup> now corrected for the systemic failures of the B3LYP method. The diethynyl-

TABLE 1. Ring Strain Enthalpies (kcal mol<sup>-1</sup>) Computed Using Group Equivalent Reactions

	B3LYP	MP2	MP2 (pred) <sup>a</sup>		B3LYP	MP2	MP2 (pred) <sup>a</sup>
<b>2</b>	51.4		33.3	<b>18</b>	25.6 <sup>b</sup>		-1.4
<b>3</b>	123.4	140.2	136.2	<b>19</b>	3.8	2.9	3.2
<b>4</b>	93.1	77.6	76.2	<b>20</b>	6.6		-6.2
<b>5</b>	58.4	36.6 <sup>c</sup>	39.5	<b>24</b>	25.4	27.1	29.1
<b>6</b>	128.7	148.5	148.3	<b>25</b>	27.0	22.3	20.8
<b>7</b>	104.9	101.3	103.2	<b>26</b>	15.3	5.4	7.4
<b>8</b>	76.4	69.8 <sup>c</sup>	75.0	<b>27</b>	23.8	26.0	28.0
<b>10</b>	76.5	61.1 <sup>c</sup>	58.5	<b>28</b>	31.1	24.9	25.4
<b>11</b>	67.1		47.2	<b>29</b>	20.5	11.8	14.0
<b>13</b>	50.4		29.4	<b>30</b>	10.4	4.7	5.1
<b>14</b>	45.4		22.1	<b>31</b>	6.4	1.2 <sup>c</sup>	-0.4
<b>15</b>	141.6	167.4	167.1	<b>32</b>	3.7	-3.0 <sup>c</sup>	-4.8
<b>16</b>	138.1		131.9	<b>33</b>	4.9	4.1	-0.1
<b>17</b>	100.7		94.9				

<sup>a</sup> Predicted using eq 1. <sup>b</sup> Estimated by the formula  $0.932 \times \Delta E_{\text{RSE}}(\text{B3LYP}) - 0.012$ . <sup>c</sup> Estimated by the formula  $0.936 \times \Delta E_{\text{RSE}}(\text{MP2}) + 0.316$ .

expanded cubane **18** and the ethynyl-expanded adamantane **20** are predicted to be strain-free!

**Deprotonation Energy (DPE).** Ring strain is well-known to correlate with enhanced acidity. The free energies for the deprotonation of propane, cyclobutane, cyclopropane, and cubane are 419.4, 408.4, 401, and 396.5 kcal mol<sup>-1</sup>, respec-



TABLE 2.  $\Delta G_{\text{DPE}}^{298}$  (kcal mol<sup>-1</sup>) of the Poly-yne

	B3LYP	MP2	MP2 (pred.) <sup>a</sup>		B3LYP	MP2	MP2 (pred.) <sup>a</sup>
<b>2</b>	317.3		327.6	<b>19</b>	402.4	401.8	403.2
<b>3</b>	380.8	374.9	375.8	<b>20</b>	327.6		336.8
<b>4</b>	328.5	337.3	337.3	<b>21</b>	371.6	377.1	375.7
<b>5</b>	301.2	316.6 <sup>c</sup>	313.2	<b>22</b>	346.8	353.7	353.5
<b>6</b>	393.4	390.2	389.6	<b>23</b>	325.9	334.1	334.8
<b>7</b>	360.8	364.5 <sup>c</sup>	362.0	<b>24</b>	405.0	404.9	403.5
<b>8</b>	347.2	351.2 <sup>c</sup>	350.0	<b>25</b>	351.0	357.4	357.3
<b>10</b>	320.0	328.2 <sup>c</sup>	329.8	<b>26</b>	326.3	337.0	335.4
<b>11</b>	312.1		323.0	<b>27</b>	406.6	405.6	406.4
<b>13</b>	304.1		316.9	<b>28</b>	370.0	373.3	374.3
<b>14</b>	297.3		309.9	<b>29</b>	350.3	356.3 <sup>c</sup>	356.8
<b>15</b>	399.2	396.9	397.3	<b>30</b>	346.2		353.1
<b>16</b>	356.1		360.9	<b>31</b>	334.9	343.5 <sup>c</sup>	343.0
<b>17</b>	340.4		347.1	<b>32</b>	323.3		332.8
<b>18</b>	297.0 <sup>b</sup>		309.4	<b>33</b>	347.4		354.1

<sup>a</sup> Predicted using eq 2. <sup>b</sup> Estimated by the formula  $0.987 \times \Delta E_{\text{DPE}}(\text{B3LYP}) - 11.73$ . <sup>c</sup> Estimated by the formula  $0.935 \times \Delta E_{\text{DPE}}(\text{MP2}) + 9.844$ .

tively.<sup>23,27,28</sup> The triple bond enhances the acidity of adjacent protons: the free energy for the deprotonation of 2-butyne is 381.7 kcal mol<sup>-1</sup>.<sup>29</sup> The combination of both ring strain and ethynyl groups inspired our previous examination of the acidity of **2**. In fact, we estimated that **2** is as acidic as methylbenzoic acid and lysine!<sup>23</sup>

To determine the deprotonation energies of the monocyclic and 3-D poly-yne, we optimized the structures of their conjugate bases at B3LYP/6-31+G(d), and some of them were also optimized at MP2/6-31+G(d). Due to the reduction in symmetry in going from the parent to the conjugate base, we were only able to compute frequencies of the smaller conjugate bases. Critical geometric parameters of optimized conjugate bases are listed in Table S2, and representative structures are displayed in Figure 2. It is readily apparent that the B3LYP and MP2 geometries are quite similar, and we will restrict ourselves to discussing the B3LYP values.

To understand the structures of the conjugate bases, it is instructive to examine the structures of a generic propargylic anion **34A** and **34B** (Chart 3). Structure **34A** presents the anion localized onto the propargylic carbon ( $C_{\text{an}}$ ). In the second structure, **34B**, an allenic system results from having the anion on the terminal sp carbon. A few important geometric changes result from this delocalization of the anionic charge: (a) the  $C_{\text{an}}-C_{\text{sp}}$  bond should have some double bond character and therefore should be rather short, (b) the  $C_{\text{sp}}-C_{\text{sp}}$  distance is longer than a typical triple bond, (d) the  $C_{\text{sp}}-C_{\text{sp}}-X$  angle should be significantly bent away from linearity, and (d) as the contribution from **34B** becomes more important, the geometry about  $C_{\text{an}}$  should become less pyramidal and more planar. As multiple triple bonds conjugate with  $C_{\text{an}}$ , delocalization occurs into these different triple bonds (see **35A-C**) and the geometric effects due to the allenic-type participation is diminished; i.e., the  $C_{\text{an}}-C_{\text{sp}}$  distance will not be as short in **35** as in **34**. The conjugate base of a pentadiyne has three major contributors, **36A-C**. Which formal  $C_{\text{sp}}$  atom is bent depends on which structure is dominant.

(27) DePuy, C. D.; Gronert, S.; Barlow, S. E.; Bierbaum, V. M.; Damrauer, R. *J. Am. Chem. Soc.* **1989**, *111*, 1968–1973.

(28) Hare, M.; Emrick, T.; Eaton, P. E.; Kass, S. R. *J. Am. Chem. Soc.* **1997**, *119*, 237–238.

(29) Gal, J.-F.; Decouzon, M.; Maria, P.-C.; Gonzalez, A. I.; Mo, O.; Yanez, M.; Chaouch, S. E.; Guillemin, J.-C. *J. Am. Chem. Soc.* **2001**, *123*, 6353–6359.

These simple geometric trends are readily apparent in the conjugate bases **21cb**, **22cb**, and **23cb**. The  $C_{\text{an}}-C_{\text{sp}}$  distance is much shorter than in the parent compounds **21–23** (see Tables S1 and S2 of the Supporting Information). This distance increases with increasing ethynyl conjugation: 1.358 Å in **21cb**, 1.390 Å in **22cb**, and 1.412 Å in **23cb**. The  $C_{\text{sp}}\equiv C_{\text{sp}}-C_x$  angle increases in the series **21cb** to **22cb** to **23cb**, further supporting the notion of the participation of added resonance structures with each ethynyl conjugating group.

The monocyclic poly-yne follow these same trends. We will focus on the two examples shown in Figure 2: **25cb** and **32cb**. Both molecules possess  $C_s$  symmetry, indicating delocalization into the  $\pi$ -bonds on both sides of the deprotonated carbon. The  $C_{\text{an}}-C_{\text{sp}}$  bond length is 1.394 Å in **25cb** and 1.384 Å in **32cb**, both shorter than this distance in their parents (1.481 Å in **25** and 1.470 Å in **32**). The  $C_{\text{sp}}-C_{\text{sp}}$  distance contracts by about 0.07 Å upon deprotonation. The  $C_{\text{sp}}\equiv C_{\text{sp}}-C_x$  angles is decidedly not linear. It is 130.2° in **25cb**, almost 30° smaller than this same bond angle in **25**. The analogous angle in **32cb** is 155.8°, some 28° smaller than in **32**. Clearly, the allenic-like resonance structure greatly participates in the description of the charge distribution of these conjugate bases. It is also interesting to note that these rings are nonplanar, reflecting again the participation of the allenic structure.

The structures of the conjugate bases of the 3-D poly-yne express the same trends. The  $C_{\text{an}}-C_{\text{sp}}$  distances are 1.35–1.40 Å, again much shorter than in the parent structures. The  $C_{\text{sp}}\equiv C_{\text{sp}}$  distances are longer than usual triple bonds. The  $C_{\text{sp}}\equiv C_{\text{sp}}-C_x$  angle is in all cases quite bent, as small as 123.9° in **4cb**. Even in the poly-yne where delocalization can occur into a diethynyl linker, a significant bending occurs at the second sp carbon, indicating significant contribution from the resonance structure **36B**. This can be seen in the structures of **5cb**, **8cb**, and **11cb** shown in Figure 2. Significant distortion from nonlinearity occurs at both the second and fourth sp carbon in all three cases.

The propensity for the anionic carbon to become planar is readily seen in Figure 2. The anionic carbon appears to move toward the interior of the cage, flattening out that corner. A simple measure of the pyramidal or planar nature of this carbon is in the sum of the bond angles about it. This sum will be 360° for a perfectly planar carbon and any pyramidal distortion will decrease the sum—a tetrahedral center will sum to 328.4°. The angle sum about the anionic carbon of **8cb** and **16cb** is small, reflecting the pyramidal nature imposed by the cyclopropyl and cyclobutyl rings. However, the angle sum is much larger when these small rings are not present; it is 349.5° in **5cb** and 351.4° in **11cb**. In fact, the anionic carbon becomes more planar as the conjugation length increases. For example, the angle sum is 327.9° in **4cb** and 349.5° in **5cb**, and the sum increases from 325.8° in **16cb** to 341.6° in **17cb** to 354.1° in **2cb** to 357.2° in **18cb**. The anionic carbon is planar (angle sum is 359.9°) in **20cb**.

Since it is clear that the propargylic anion is delocalized into every adjacent triple bond, it is reasonable to expect that the deprotonation energies of the 3-D poly-yne will be much smaller than typical hydrocarbons. Before discussing the deprotonation free energies ( $\Delta G_{\text{DPE}}^{298}$ ) listed in Table 2, we must discuss computational methods. MP2/6-31+G\* DPEs are in excellent agreement with experiment for many hydrocarbons. For example, the experimental<sup>23,27,28</sup> and MP2  $\Delta G_{\text{DPE}}^{298}$  are 408.4 and 405.6 kcal mol<sup>-1</sup> for cyclobutane, 401 and 404.9 kcal mol<sup>-1</sup> for cyclopropane, and 396.5 and 396.9 kcal mol<sup>-1</sup> for

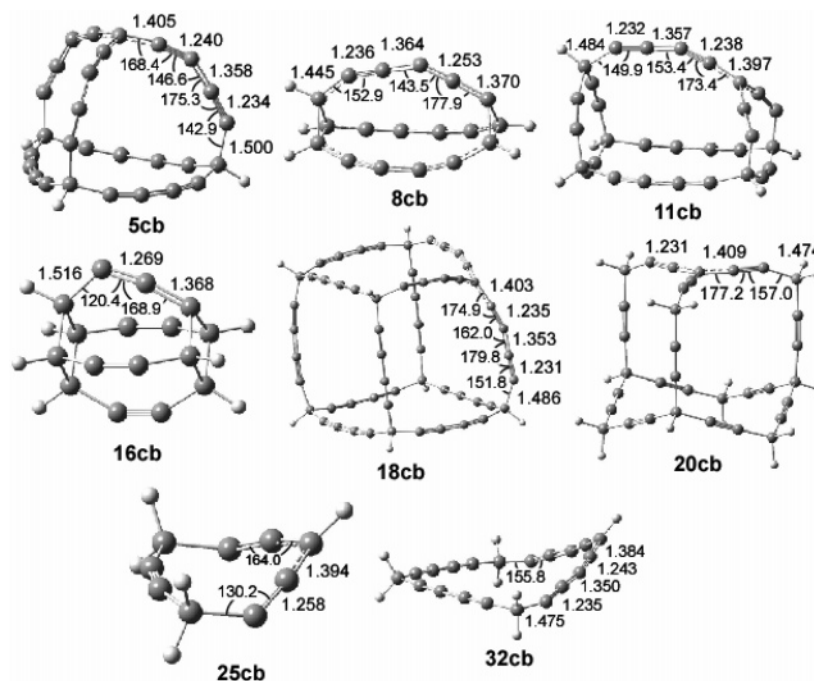
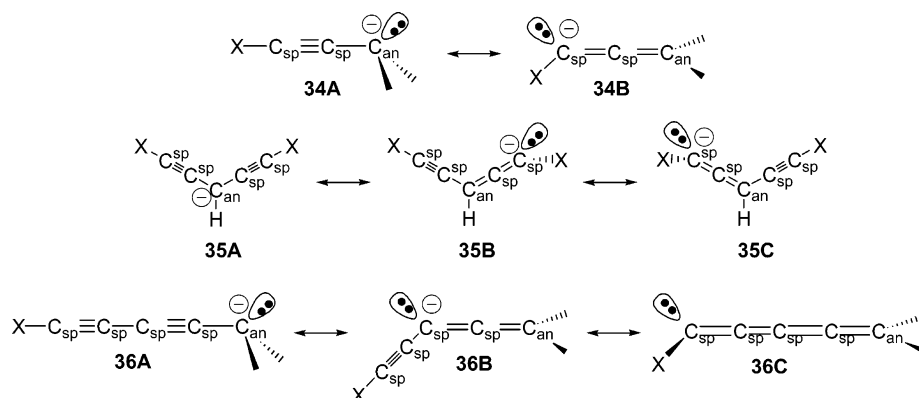


**FIGURE 2.** Representative B3LYP/6-31+G(d)-optimized structures of the conjugate bases of monocyclic and cage poly-yne. All distances are in Å and all angles are in degrees.

### CHART 3



cubane. B3LYP/6-31+G\*, on the other hand, fares much worse in predicting DPEs, with errors greater than  $5 \text{ kcal mol}^{-1}$ . Given the computational limitations due to the size of many of the molecules we are interested in, we are forced to make use of B3LYP.

This could be potentially problematic. Woodcock et al.<sup>30</sup> noted that DFT (in particular, B3LYP, BLYP, and BP86) inverts the relative energy of cumulenes and alkynes. For example, B3LYP/6-311G predicts that allene is  $1.5 \text{ kcal mol}^{-1}$  lower in energy than propyne, when in fact propyne is  $1.4 \text{ kcal mol}^{-1}$  more stable than allene. Regardless of the basis sets [6-31G to 6-311++G(2df,2pd)] or the functional (B3LYP, BLYP, and BP86), DFT predicts allene to be more stable than propyne, and the same is true for the next two larger homologues. Since the poly-yne conjugate bases express allenic character, the proclivity for DFT to incorrectly treat the competition between cumulene and alkyne may result in incorrect DPEs. However, Woodcock et al. also demonstrated that MP2 predicts the correct

energetic ordering (alkyne more stable than cumulene), though it overestimates the stability of the alkyne. Thus, we plan to correct our B3LYP DPE values by comparing them to the MP2 values for a limited set of compounds.

The B3LYP values of  $\Delta G_{\text{DPE}}^{298}$  tend to be below those predicted at MP2 (Table 2). In fact, a quite reasonable correlation exists between them, and we made use of this correlation in an earlier paper.<sup>7</sup> In analogy with eq 1, however, we have obtained a multiple regression relationship between the B3LYP and MP2 values of  $\Delta G_{\text{DPE}}^{298}$  shown in eq 2.

$$\Delta G_{\text{DPE}}^{298}(\text{MP2, predicted}) = 0.897\Delta G_{\text{DPE}}^{298}(\text{B3LYP}) - 2.031N_{3\text{MR}} - 0.509N_{4\text{MR}} + 0.062N_{\text{trip}} + 42.28 \quad (2)$$

The correlation is outstanding ( $r^2 = 0.998$ ) and affords excellent estimates of the full range of molecules examined here. Table 2 lists the computed B3LYP and MP2 values of the free energy of deprotonation along with the predicted values using eq 2. We will use either the actual MP2 values or the predicted values from eq 2 in the discussion that follows.

(30) Woodcock, H. L.; Schaefer, H. F.; Schreiner, P. R. *J. Phys. Chem. A* **2002**, *106*, 11923–11931.

We begin by examining the series **21**–**23**, which explores the effect of delocalization of the anion into one, two, or three separate ethynyl groups. The DPE for the removal of a proton from the terminal carbon of propane is 407.6 kcal mol<sup>-1</sup>. The DPEs decrease from 377.1 kcal mol<sup>-1</sup> for **21** to 353.7 kcal mol<sup>-1</sup> for **22** to 334.1 kcal mol<sup>-1</sup> for **23**. The effect of the first ethynyl group is to decrease the DPE by 30.5 kcal mol<sup>-1</sup>, the second ethynyl group lowers the DPE by another 23.4 kcal mol<sup>-1</sup>, and the third ethynyl group decreases it by another 19.6 kcal mol<sup>-1</sup>. Since all of these conjugate bases are planar about the formal carbanion center, full conjugation is possible, so the diminishing effect of each subsequent alkynyl group is due to the diminished relative delocalization afforded by sequential substitution.

The DPEs of **25** and **30** should be similar to that of **22** in that the anion can delocalize into two different ethynyl groups. In fact, the DPE of **30** is 0.4 kcal mol<sup>-1</sup> less than that of **22**, indicating that the nonconjugating ethynyl groups are not affecting the DPE. **25** is slightly less acidic, reflecting the fact that there is some strain in **25cb** that reduces the charge delocalization.

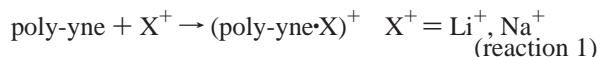
Delocalization of the anion into a neighboring diethynyl group should stabilize the anion to a greater extent than that afforded by a neighboring ethynyl group. This is seen in the much lower DPE for **29** (356.3 kcal mol<sup>-1</sup>) than for **28** (373.3 kcal mol<sup>-1</sup>). Similarly, the DPE of **26** is 20.4 kcal mol<sup>-1</sup> less than that of **25**. The lowest DPE (332.8 kcal mol<sup>-1</sup>) for a monocyclic poly-yne is that of **32**, where the anion can delocalize into two adjacent diethynyl groups.

The DPEs of the 3-D poly-yynes are remarkable in that many of them are predicted to be extraordinarily acidic. We had already reported the very low DPE computed for **2**. Our revised estimate of its DPE is 327.6 kcal mol<sup>-1</sup>. This very low DPE comes from the delocalization of the anion into the three neighboring ethynyl groups and from the high sp character of the C–H bond. However, **2** is not the most acidic of the 3-D poly-yynes. A 3-D poly-yne that is more strained than **2** will have even more sp character. Both **4** and **10** are more strained than **2** yet have the same number of adjacent ethynyl groups. Both are *less* acidic than **2**, and this reduced acidity must come from poorer delocalization into the alkynyl groups. Maximal delocalization into the three neighboring alkynyl groups occurs if the groups are coplanar with the anionic center. The angle sum about the anionic carbon increases in the series **4** < **10** < **2**, which parallels their relative acidities. The effect of strain on DPE is seen in the much lower DPE of **2** than **20**, even though the anion of the latter is planar.

The acid-enhancing effect of a neighboring diethynyl group is substantial, as seen in the comparison the DPEs of **28** and **29** or of **16** and **17**. Thus, it is not surprising that the most acidic 3-D poly-yynes are ones that have three diethynyl groups that can effectively conjugate with the carbanion center. The DPE of **5** is 313.2 kcal mol<sup>-1</sup> and that of **14** is even lower, 309.9 kcal mol<sup>-1</sup>. The difference in DPEs of these two compounds comes again from the better ability of the larger, less strained molecule to adopt a near planar arrangement about the carbanion center. The acidity of **14** is similar to that of 2,4,6-trinitrotoluene and 2,3-dinitrophenol.<sup>23</sup> The per-diethynyl expanded cubane **18** and the per-diethynyl expanded prismane **14** are extraordinarily acidic, with DPEs of about 309 kcal mol<sup>-1</sup>. To put this into perspective, these DPEs are comparable to that of TNT and 2,3-dinitrophenol!<sup>23</sup>

**Cation Affinities.** We noted in our earlier work that the poly-yynes **2** and **30** can effectively complex cations by coordination of the cation with the  $\pi$ -bonds.<sup>7</sup> Cation coordination to the poly-yynes examined here allows for explication of the best size of the ring or cage to capture a lithium or sodium cation.

We optimized the structure of the complexes between many of the poly-yynes and either Li<sup>+</sup> or Na<sup>+</sup> at B3LYP/6-31+G(d) and MP2/6-31+G(d). Generally, three different initial geometries were attempted for the cation complexes with a poly-yne cage: (1) with the cation at the center of the cage, (b) with the cation at the center of a face, and (c) with the cation located above a face, outside the cage. For the complexes with the poly-yne rings, two geometries were attempted, with the cation at the center or above the center of the ring. Analytical frequency analysis identified local minima, and when imaginary frequencies were found, the cation was displaced in accordance with that frequency, reducing the symmetry of the complex. Representative structures are drawn in Figure 3. Computed cation affinities, defined as the energy associated with reaction 1, are listed in Table 3.



Optimal interaction of the cation with the poly-yne occurs when the cation can effectively interact with as many alkynyl units as possible. This is achieved by positioning the cation at an appropriate distance to maximize electrostatic attractions while steric interactions are minimized. As a gauge of this “ideal” distance, the B3LYP/6-31+G(d)-optimized C–Li distance is 2.33 Å in the Li<sup>+</sup>acetylene complex and the C–Na distance is 2.70 Å in the Na<sup>+</sup>acetylene complex.

The series of complexes **29Li**, **30Li**, and **32Li** nicely demonstrates how this “ideal” distance is achieved between as many alkynyl units and the Li<sup>+</sup> as possible. The cross ring C···C distance in **29** is 3.585 Å, too small to fit the Li<sup>+</sup>. Instead, the cation lies above the ring and is therefore only weakly interacting with the more distant carbon atoms of the diethynyl groups. On the other hand, the cross ring C···C distance in **30** is 4.748 Å. Situating the lithium cation at the center of this ring affords a nearly ideal C–Li distance. In fact, the alkynyl groups actually distort inward toward the cation relative to their position in the free ring. All four alkynyl groups strongly interact with the cation in **30Li**, but in **29Li** these interactions are weaker due to the longer separations. This leads to a larger cation affinity for **30Li** ( $\Delta G_{\text{CA}}^{298} = -52.0$  kcal mol<sup>-1</sup>) than for **29Li** ( $\Delta G_{\text{CA}}^{298} = -42.1$  kcal mol<sup>-1</sup>). **32**, being larger than **30**, can easily accommodate the cation in its interior. However, if it sits in the center of the ring, the C–Li distance would be too long (~4.7 Å). Instead of being at the ring center, and having very weak interactions with all eight of the alkyne groups, the lithium cation moves toward one corner, resulting in a structure with C<sub>2v</sub> symmetry. The cation achieves “ideal” separation from the two ethynyl groups adjoining the saturated carbon. Since the cation really interacts with just these two alkynyl groups, the cation affinity of **32Li** ( $\Delta G_{\text{CA}}^{298} = -39.0$  kcal mol<sup>-1</sup>) is less than that of **30Li**, where the cation interacts with four alkynyl groups. Since the “ideal” C–Na distance is longer than the C–Li distance, the sodium cation sits above the ring in both **29Na** and **30Na** and off-center in **31Na**, like where lithium is positioned in **32Li**. It does sit very close to the ring center of **31Na**, only slightly distorted from D<sub>2h</sub> to C<sub>2v</sub> symmetry. The **33Na** complex has no symmetry (C<sub>1</sub>).



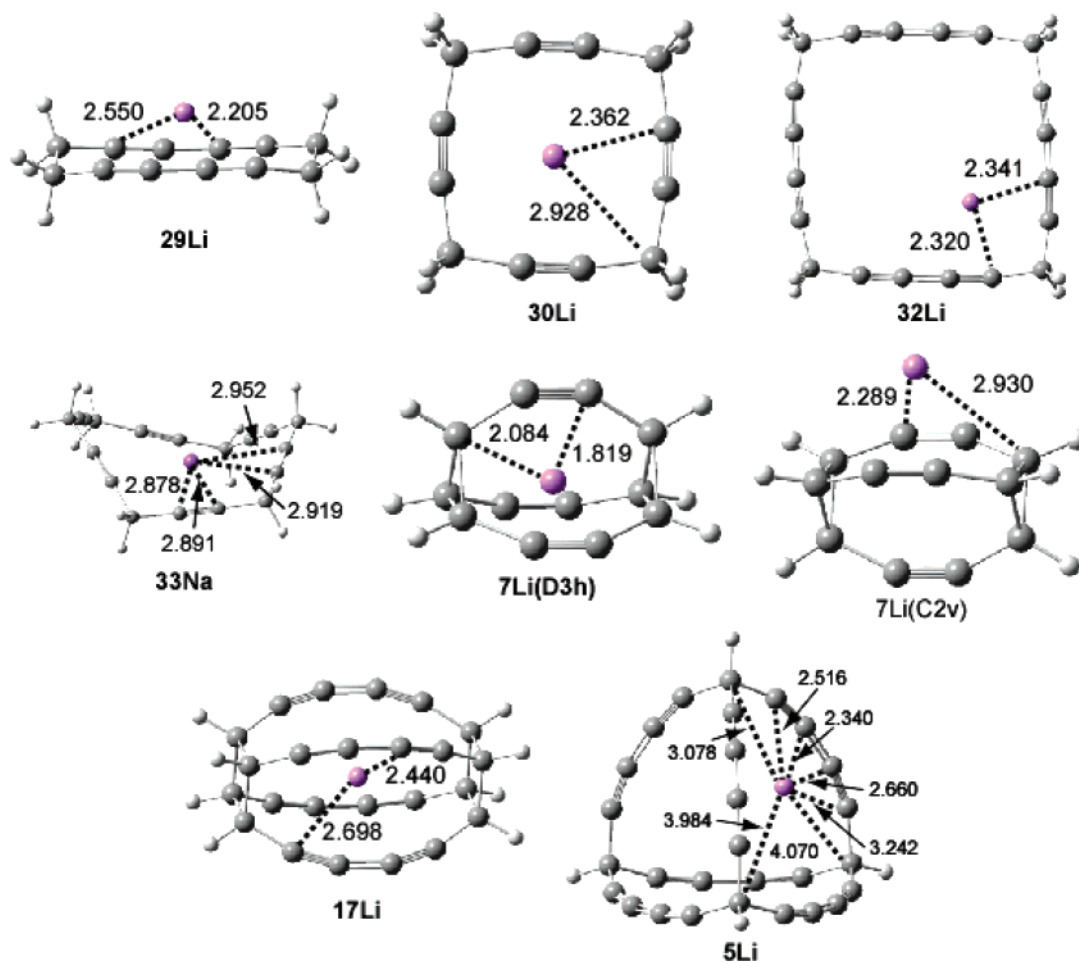


**FIGURE 3.** Representative B3LYP/6-31+G(d) structures of the complexes between lithium or sodium cation with cyclic or cage poly-yynes. All distances are in angstroms and all angles are in degrees.

**TABLE 3.** Lithium and Sodium Cation Affinities ( $\text{kcal mol}^{-1}$ ) of the Poly-yynes

	$\Delta E_{\text{CA}}(\text{DFT})$	$\Delta G_{\text{CA}}^{298}(\text{DFT})$	$\Delta E_{\text{CA}}(\text{MP2})$		$\Delta E_{\text{CA}}(\text{DFT})$	$\Delta G_{\text{CA}}^{298}(\text{DFT})$	$\Delta E_{\text{CA}}(\text{MP2})$
25Li	-41.6	-32.0	-42.6	25Na	-27.2	-18.5	-28.3
26Li	-46.9	-40.7	-47.9	26Na	-38.5	-31.1	-39.7
28Li	-37.8	-29.6	-36.6	28Na	-24.6	-17.0	-23.6
29Li	-50.5	-42.1	-50.0	29Na	-33.7	-26.1	-33.4
30Li	-61.9	-52.0	-64.4	30Na	-40.6	-31.6	-42.4
31Li	-55.4	-47.1	-56.5	31Na	-42.0	-35.9	-42.4
32Li	-45.6	-39.0		32Na	-35.0	-29.0	
33Li	-53.6	-46.4		33Na	-46.6	-38.8	
4Li	-26.7	-15.1	-33.0	4Na	49.9	62.0	
5Li	-41.0	-35.2		5Na( $T_d$ )	-31.6	-22.2	
7Li( $D_{3h}$ )	29.9	40.6	32.2	5Na( $C_{3v}$ )	-33.1	-26.7	
7Li( $C_{2v}$ )	-42.7	-35.0		7Na( $D_{3h}$ )	177.9	187.3	192.3
8Li	-54.1	-43.1	-55.9	7Na( $C_{2v}$ )	-29.8	-22.7	
10Li	-51.7	-43.6	-56.8	8Na	-11.2	0.8	-9.0
11Li	-47.2	-38.5 <sup>a</sup>		10Na	-39.2	-28.7	
16Li	-12.1	-1.2		11Na	-39.0	-30.4 <sup>b</sup>	
17Li	-60.7	-50.3		16Na	90.7	101.5	
2Li	-58.1	-49.7 <sup>a</sup>		17Na	-34.8	-24.6	
				2Na	-46.2	-37.7 <sup>b</sup>	

<sup>a</sup> Estimated by the formula  $1.026 \times \Delta E_{\text{CA}}(\text{B3LYP}) + 9.996$ . <sup>b</sup> Estimated with the formula  $1.012 \times \Delta E_{\text{CA}}(\text{B3LYP}) + 9.038$ .

These same considerations dictate the structure of the complexes formed between a cation and a 3-D poly-yne. The lithium cation can, in principle, be placed in the center of the cage of **7**, forming **7Li( $D_{3h}$ )**. The interior of **7** is, however, too small to accommodate the lithium cation, and the resulting C–Li distance is too short, only 1.819 Å. This is reflected in its cation

affinity of  $+40.6 \text{ kcal mol}^{-1}$ ; the complex **7Li( $D_{3h}$ )** is unstable relative to separated reactants. Rather, lithium cation will complex with one of the *faces* of **7** to give **7Li( $C_{2v}$ )**. In this complex, the C–Li distance is near its “ideal” value. The cation affinity of **7Li( $C_{2v}$ )** is slightly less than the cation affinity of **28Li**, the complex of the “face” of **7** with  $\text{Li}^+$ . The cavity of



TABLE 4. Electronic Excitation Energies for Some Reference Alkynes<sup>a</sup>

compound	computed lowest state		computed first visible states		expt <sup>b</sup> nm
	eV	nm	eV	nm	
acetylene	6.655	186.3	7.703	161.0(0.089)	
	<i>6.706</i>	<i>184.9</i>	8.974	138.2(0.446)	
			<i>8.581</i>	<i>144.5(0.398)</i>	
1-butyne	6.381	194.3	6.552	189.2(0.024)	
			8.480	146.2(0.263)	
			6.676	185.7(0.033)	
<b>23</b>	6.309	196.5	8.002	154.9(0.176)	
			6.567	188.8(0.031)	
			7.765	159.7(0.104)	
<b>22</b>	6.298	196.8	6.567	188.8(0.031)	
			7.765	159.7(0.104)	
			7.479	165.8(0.044)	
2-butyne	6.201	200.0	7.479	165.8(0.044)	
			7.786	159.2(0.253)	
			7.101	174.6(0.027)	
1,3-butadiyne	4.704	263.6	7.101	174.6(0.027)	144.6
	<i>4.669</i>	<i>265.5</i>	7.267	170.6(1.160)	
			<i>6.916</i>	<i>179.2(1.034)</i>	
1,3-pentadiyne	4.667	265.7	6.714	184.6(0.012)	
			7.162	173.1(1.346)	
			7.075	175.2(0.193)	
2,4-hexadiyne	4.654	266.4	7.297	169.2(2.199)	
			4.717	262.9(0.014)	
			6.961	178.1(2.187)	
1,3,6,8-nonatetrayne	4.543	272.9	4.641	267.0(0.023)	
			6.347	195.3(0.536)	
			6.341	195.5(2.578)	
5-(1,3-butadiynyl)-1,3,6,8-nonatetrayne	4.538	273.2	4.641	267.0(0.023)	
			6.347	195.3(0.536)	
			6.341	195.5(2.578)	
1,3,5-hexatriyne	3.696	335.4	6.341	195.5(2.578)	183.1
	<i>3.618</i>	<i>342.7</i>	6.028	205.7(2.368)	
	3.670	337.8	6.219	199.4(2.870)	
1,3,5-heptatriyne	3.670	337.8	6.219	199.4(2.870)	
	3.662	338.6	6.207	199.8(3.688)	
	3.095	400.6	5.538	223.9(3.704)	
2,4,6-octatriyne	3.095	400.6	5.538	223.9(3.704)	207.3
	2.988	414.9	5.230	237.0(3.350)	

<sup>a</sup> TD-B3LYP/6-31+G(\*) values in normal type, TD-BLYP/6-31+G(d)/B3LYP/6-31+G(d) values in italics, oscillator strength in parenthesis. <sup>b</sup> Reference 36.

the cage poly-yne **17** is large enough to accommodate a lithium cation. The distance between the cation and the interior sp carbon atoms is 2.440 Å, indicating a strong interaction between them. It is thus not surprising that its cation affinity is quite large ( $-50.3$  kcal mol<sup>-1</sup>). The poly-yne **5** is also sufficiently large enough to hold a lithium cation in its interior. However, as in **32**, the interior is *too* big; the distance from the cage center to the closest sp carbon is 3.23 Å. The most stable complex is formed with the cation in one of the faces (**5Li**) and not in the center of that face but shifted toward one corner to achieve the “ideal” distance with two of the alkynyl groups. Its cation affinity ( $-35.2$  kcal mol<sup>-1</sup>) is similar to that of **32Li**, which mimics the complexing face of **5Li**. Similarly, the sodium cation sits in one of the faces in **5Na**. We have seen this same behavior in the complexes with **2**.<sup>7</sup> The most favorable configuration of **2Li** has the cation in one of the faces; the structure where it sits in the center of the cube has three imaginary frequencies, each corresponding to motion of the lithium toward one of the faces. However, since Na<sup>+</sup> is larger than Li<sup>+</sup>, sodium cation is well accommodated in the center of the cage.

We now turn to the values of the cation affinities ( $\Delta E_{CA}$ ) listed in Table 5. Unlike for the RSEs and DPEs, the cation affinities do not suffer from a significant methodological dependency. The only serious disagreement between the B3LYP and MP2  $\Delta E_{CA}$  values is for **7Na(D<sub>3h</sub>)**, a structure that is seriously strained. Otherwise, the two methods are in excellent agreement, reflective of the interaction being largely electrostatic in nature.

There is basis set dependence. We had previously computed  $\Delta G_{CA}^{298}$  at B3LYP/6-31G\* for **2Li** and **30Li** as  $-60.3$  and  $-60.0$  kcal mol<sup>-1</sup>, respectively. These values are reduced to  $-49.7$  and  $-52.0$  kcal mol<sup>-1</sup> at B3LYP/6-31+G(d). These differences are due in large part to the reduction in basis set

TABLE 5. TDDFT/B3LYP/6-31+G(d) Excitation Energies for the Poly-yne and Their Conjugate Bases<sup>a</sup>

compd	computed energy (eV)	compd	computed energy (eV)
<b>25</b>	5.447	<b>25cb</b>	2.642
	5.892(0.071)		
<b>26</b>	3.714	<b>26cb</b>	2.106
	4.538(0.020)		
<b>28</b>	5.027	<b>28cb</b>	2.217
	5.860(0.020)		
<b>29</b>	4.207	<b>29cb</b>	2.108
	5.212(0.010)		
<b>30</b>	5.358	<b>30cb</b>	2.708
	6.187(0.033)		
<b>31</b>	4.364	<b>31cb</b>	2.410
	4.190		
<b>32</b>	4.602(0.031)	<b>32cb</b>	1.900
	6.085		
<b>33</b>	6.288(0.119)	<b>33cb</b>	1.831
	4.482		
<b>4</b>	4.482	<b>4cb</b>	2.738
<b>5</b>	3.273	<b>5cb</b>	2.236
<b>7</b>	4.046	<b>7cb</b>	2.523
<b>8</b>	3.530	<b>8cb</b>	2.226
<b>10</b>	4.665	<b>10cb</b>	2.764
<b>11</b>	4.192	<b>11cb</b>	2.357
<b>13</b>	3.552	<b>13cb</b>	1.778
<b>14</b>	3.771	<b>14cb</b>	1.617
<b>16</b>	4.068	<b>16cb</b>	1.944
<b>17</b>	3.737	<b>17cb</b>	1.728
<b>2</b>	4.780	<b>2cb</b>	2.695
<b>20</b>	5.943		

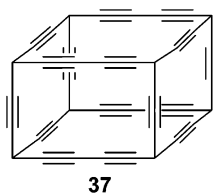
<sup>a</sup> Oscillator strength in parenthesis.

superposition error. Further increase in the basis set size will lead to further decrease in the cation affinity energies, though we expect that the further decrease is likely to be only a few kilocalories per mole.

The positive cation affinity energy values occur when the cation is forced into a molecular interior that is too small. Instead of being in this cavity, the cation will complex to a face, such as in the structures of the lithium or sodium complexes with **7**. While we have not optimized the face-complexed analogues of the center-complexes **4Na** or **16Na**, they undoubtedly will be stable, with negative values for their cation affinity energies. **16Li** is a stable structure with the cation in the cage center, but the (uncomputed) structure with the cation associated with a face will likely be lower in energy.

The most effective cyclic poly-yne hosts for  $\text{Li}^+$  are **29–31**. The cation sits in the center of each ring and can interact with multiple alkynyl groups. The 3-D poly-yne **2** is also a good host, using the analogous face of **30** to hold the cation. **17** is a slightly better host than **2**; in this case the cation sits in the interior of the ring and can interact with all of the alkynyl groups. While the lithium cation does occupy the cage center in the complexes with both **8** and **10**, neither is as good a host as when the cation binds to a face, like **30Li**. In **8Li**, the cation is too far from the terminal carbons of the diethynyl groups, and in **10**, the cage interior is just a bit too large. Expanding the size of the ring or cage beyond what we have examined here will not improve the complexation ability. Larger systems will possess interiors that are simply too big for the lithium cation, which will then have to coordinate off-center to achieve “ideal” interaction distances with only some of the alkynyl groups.

The best cyclic poly-yne hosts for  $\text{Na}^+$  are **31** and **33**. These large rings suggest that only the largest of the 3-D poly-ynes will be useful hosts for sodium cation. In fact, the only 3-D poly-yne with cation affinity energy competitive with that of these two rings is **2**. The cavity of **2** is sufficiently large to hold the sodium cation within its interior. The expanded cubane **37**, slightly larger than **2**, might also host  $\text{Na}^+$  in its interior,



while **18** and **20** will likely complex the sodium cation within a face.

**Electronic Excitation Energy.** Perhaps the major interest in the poly-ynes, and especially the 2-D and 3-D poly-ynes, is their potential use in electrooptical devices. Our interest here is how the first electron excitation energy varies with increasing number of ethynyl groups in multiple dimensions and in different geometries. To compute the energy difference between the ground and first excited state, we use the time-dependent density functional method (TDDFT), employing the B3LYP functional and the 6-31+G(d) basis set, which provides the vertical excitation energy.

TDDFT has been used for predicting the excitation energy of some organic systems, generally providing excitation energies that are 0.4 eV or more too small, though trends and state ordering are reproduced.<sup>31–34</sup> Claims of more serious errors in

the TDDFT computation of excited states of poly-acenes were made by Grimme and Parac.<sup>35</sup>

We begin here with a study of simple alkynes and linear poly-ynes to test the performance of this methodology. Table 4 presents the calculated vertical excitation energies of 14 alkynes, five having an isolated triple bond, five with one or two isolated diethynyl groups, three with a triethynyl group, and one with a tetraethynyl group. The lowest energy transition invariably has no oscillator strength. Therefore, we also list the first transition with an oscillator strength greater than 0.01 and also the first intense transition (if there is one within the first 20 or so excited states).

The experimental data absorption energy is sparse for these small alkynes.<sup>36</sup> The computed B3LYP values of the wavelength for the transition in 1,3-butadiyne, 1,3,5-hexatriyne, and 1,3,5,7-octatetrayne are too large by 12–30 nm. Similar errors are also seen when the BLYP functional is used (see the values in italics in Table 4).

Given that these computed values cannot be used to predict actual transition energies, can they provide trends? Our real interest is in determining if isolated alkynyl groups oriented in different directions can interact, leading to changes in their excitation energies. In other words, will the different poly-yne geometries expressed in compounds **2–20** exhibit differing excitation energies?

Trends in the excitation energy are readily discernible from the computational results in Table 4. The energy for the lowest energy transition is about 6.3 eV for monoalkynes, 4.6 eV for dialkynes, 3.6 eV for trialkynes, and 3.1 eV for tetralkynes. This trend is in accord with the simple particle-in-a-box concept that as the delocalization length increases, the spacing between energy states decreases. The same trend in decreasing energy with increasing chain length is seen with the first intense excitation: about 7.8 eV for monoalkynes, 7.1 eV for dialkynes, 6.1 eV for trialkynes, and 5.2 eV for tetralkynes. This is the trend observed in both experimental<sup>36,37</sup> and computed<sup>38</sup> excitation energies of polyalkynes. So while absolute excitation energies may be poorly predicted, TDDFT does correctly indicate that the excitation energies of the triethynyl compounds are less than that of the diethynyl compounds, which are less than that of the monoethynyl compounds, as also found by Zahradnik.<sup>34</sup> Trends in the excitation energies of the ring and cage poly-ynes should therefore be obtainable.

The computed lowest excitation energies for the monocyclic and 3-D poly-ynes and their conjugate bases are listed in Table 5. Also, listed is the lowest excitation energy with an oscillator strength greater than 0.01 for the monocyclic poly-ynes. (No cage poly-yne exhibited an excitation with an oscillator strength above 0.01 within the first 14 states.)

Looking first at the monocyclic poly-ynes **25–33**, it is readily apparent that **33** is an outlier. Its lowest excitation energy (6.085 eV) is much higher than for the other cyclic polynes. In fact, this excitation energy is quite similar to that of the reference

(33) Fabian, J.; Diaza, L. A.; Seifert, G.; Niehaus, T. *J. Mol. Struct. (THEOCHEM)* **2002**, *594*, 41–53.

(34) Zahradnik, R.; Srnec, M.; Havlas, Z. *Collect. Czech. Chem. Commun.* **2005**, *70*, 559–578.

(35) Grimme, S.; Parac, M. *ChemPhysChem* **2003**, *4*, 292–295.

(36) Kloster-Jensen, E.; Haik, H. J.; Christen, H. *Helv. Chim. Acta* **1974**, *57*, 1731–1744.

(37) Grutter, M.; Wyss, M.; Fulara, J.; Maier, J. P. *J. Phys. Chem. A* **1998**, *102*, 9785–9790.

(38) Scemama, A.; Chaquin, P.; Gazeau, M.-C.; Bénilan, Y. *Chem. Phys. Lett.* **2002**, *361*, 520–524.

(31) Bauernschmitt, R.; Ahlrichs, R. *Chem. Phys. Lett.* **1996**, *256*, 454–464.

(32) Bauernschmitt, R.; Ahlrichs, R.; Hennrich, F. H.; Kappes, M. M. *J. Am. Chem. Soc.* **1998**, *120*, 5052–5059.

alkynes, like **22**. The alkynyl groups of **33** are noninteracting. On the other hand, the remaining monocyclic poly-yynes can be separated into two categories: those with isolated ethynyl groups and those with isolated diethynyl groups. Compounds **25**, **28**, and **30**, with formally isolated ethynyl groups, have first excitation energies from 5.0 to 5.4 eV. This is about 1 eV less than the value of the standard mono-yynes (Table 4), 6.3 eV. Their lowest visible transition energy is about 6 eV, again less than the value for the standards, 7.8 eV. Compounds **26**, **29**, **31**, and **32**, with formally isolated diethynyl groups, have first excitation energies from 3.7 to 4.2 eV, again smaller than the value of standard acyclic diethynyl compounds, 4.6 eV. Their lowest visible transition energy is 4.5 to 5.2 eV, less than the standard value of about 7 eV.

The values for both the lowest excitation energy and the first visible transition of the cyclic poly-yynes (other than **33**) deviate from the values of the acyclic standards. This reflects the fact that interaction between the triple bonds increases the delocalization length, reducing the gaps between energy levels. Transitions with reasonable oscillator strengths were not seen among the lowest 14 states of the larger poly-yynes. We will therefore discuss only the values of the lowest excitation energy for the remaining molecules, since the trends here should mimic the trends of the visible transitions as well.

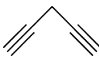
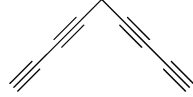
The cage poly-yynes with isolated ethynyl groups (**4**, **7**, **10**, **16**, and **2**) have excitation energies from 4.0 to 4.8 eV, smaller than the analogous cyclic poly-yynes. The outlier is the expanded adamantane **20**, which has its excitation energy (5.9 eV) just slightly below that of standard alkynes. The cage poly-yynes with isolated diethynyl groups (**5**, **8**, **11**, **13**, **14**, and **17**) have excitation energies from 3.2 to 4.2 eV, comparable to the values of their monocyclic analogues. Most importantly, all of these poly-yynes exhibit excitation energies smaller than those of the acyclic standards (Table 4).

What leads to the lowered excitation energy in the poly-yynes relative to the acyclic reference compounds? The seemingly isolated ethynyl and diethynyl groups must be interacting with each other, effectively increasing the delocalization length of the  $\pi$ -system.

Unfortunately, there are no simple measures of this “effective” delocalization length nor the factors that correlate with engendering greater interaction between the isolated alkynyl groups. For example, for the series **30**, **31**, and **32**, their excitation energies decrease in that order, which parallels the potential delocalization length if one simply counts all of the triple bonds, i.e., four in **30**, six in **31**, and eight in **32**. This is also true in comparing **25** with **30**, but not for the pairs **26** with **32** or **8** with **17**. Obviously, **33** also defies this explanation.

Another simple suggestion is that the closer are the alkynyl units, the more they will interact, leading to a lower excitation energy. This is the case for the comparison of **26** with **32**, where the closest distance between sp carbons is 2.37 and 2.41 Å, respectively. However, the distance is greater in **30** (2.39 Å) than in **26** (2.30 Å), but the transition energy of **30** is smaller than for **26**. Nonetheless, there is some underlying dependence of the transition energy on the distance separating the isolated alkyne groups. We computed the transition energies of 1,4-pentadiyne and 1,3,6,8-nonatriyne with the angle about the saturated carbon constricted to that found in **25** for the former and **26** for the latter (see Table 6). Changing the angle about the saturated carbon of 1,4-pentadiyne from 113.7° to 101.7° (the angle in **25**) diminishes the excitation energy by about 0.1

TABLE 6. TDDFT/B3LYP/6-31+G(d) Excitation Energies of Different Geometries of 1,4-Pentadiyne and 1,3,6,8-Nonatriyne

geometry		
optimized	6.30	4.54
constrained about sp <sup>3</sup> C atom	6.18	4.56
constrained about all C atoms	5.25	4.25

eV. For 1,3,6,8-nonatriyne, the change in this angle from 113.4° to 106.9° causes effectively no change in the excitation energy. Therefore, the role of distance is important only when the  $\pi$ -bonds are brought fairly close together.

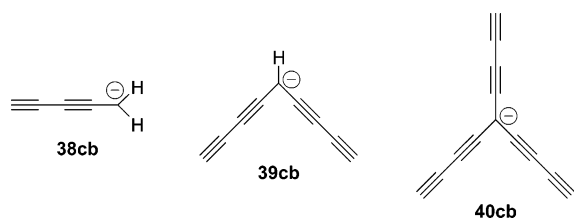
Interestingly, further distorting of 1,4-pentadiyne and 1,3,6,8-nonatriyne to have the angle about the sp carbon atoms as in the cyclic poly-yne reference produces a large effect on the transition energies. For 1,3,6,8-nonatriyne, where the angles about the sp carbon atoms are changed from 180° to 165.2° and 171.4° nets a reduction of 0.3 eV. The effect is especially dramatic for 1,4-pentadiyne: constricting the angle about the sp carbons to 159.1° gives an excitation energy that is a full electronvolt below that of fully relaxed 1,4-pentadiyne.

The angular distortion somewhat weakens the  $\pi$ -bond in the plane of the distortion, which should result in a lowering of the excitation energy. This alone does not account for the excitation energies in the poly-yynes, which have excitation energies even less than what the bending alone will produce. Therefore, the formally isolated triple bonds of the ring and cage poly-yynes are interacting through space with each other. On the other hand, both **20** and **33** act as ordinary alkynes, which have no significant interaction between their alkynyl groups nor any bending about the sp carbons, very much unlike the other cyclic and cage poly-yynes examined here.

We next turn our attention to the excitation energies of the conjugate bases of the poly-yynes, whose values are listed in Table 5. A few simple trends can be discerned by examining related molecules. First we look at the poly-yynes made of isolated ethynyl linkers. The excitation energies of the conjugate bases of **21**, **22**, and **23** are 2.78, 3.01, and 3.13 eV, respectively. This may appear counterintuitive: the excitation energy increases with the apparent delocalization length. However, the conjugate base of propyne is really best understood as dominated by resonance structure **34B**, so its excitation is really more  $n \rightarrow \pi^*$ . The importance of the resonance structure with the negative charge on the deprotonated carbon is greater in **22cb** and greater still in **23cb**, suggesting their increasing  $\pi \rightarrow \pi^*$ . This is reflected in the terminal C–C–H angles that increase from 122.0° in **20cb** to 141.5° in **21cb** to 160.3° in **22cb**.

The cyclic and cage poly-yynes analogous to **21cb**–**23cb** have excitation energies smaller than these acyclic references. For example, the excitation energies of **2cb**, **4cb**, and **10cb** are all about 0.4 eV less than that of their analogue **23cb**. This diminishment of the excitation energy is similar to that discussed for the parent poly-yynes and suggests that the (delocalized) anion is interacting with the other alkynyl groups in the molecule. This occurs even in the series **21cb**, **7cb**, **28cb**, and **17cb**, where the anion is largely localized on the sp<sup>2</sup> carbon as in **34B**. The excitation energy of **17cb** is 0.82 eV smaller than that of **21cb**, even though both have very similar angles about the anionic sp<sup>2</sup> carbon.

The trend in the excitation energies of **38cb**, **39cb**, and **40cb** are 2.63, 2.33, and 2.50 eV, respectively. **38cb** has appreciable



character of **36C** (the terminal C–C–H angle is 134.3°), while **39cb** and **40cb** are best described as analogous to **36A**; i.e., the former has appreciable  $sp^2$  anionic character, while the latter two are delocalized  $\pi$ -anions. As with the conjugate bases of the ethynyl polyenes, the conjugate bases of the cyclic and cage diethynyl poly-yne have excitation energies reduced from their acyclic references. For example, the excitation energies of **5cb** and **14cb** are less (in the latter case, much less) than that of **40cb**. Again, this reflects interaction of the isolated alkynyl groups with the anion.

As demonstrated in Table 5, the excitation of the poly-yne spans a broad range of energies. Clearly, these ring and cage poly-yne offer a great opportunity for creating molecules with selected absorptions, tuned for specific applications.

## Conclusions

Ethynyl- and diethynyl-expanded cage structures exhibit a number of properties that make them interesting synthetic targets. In this article, we presented B3LYP/6-31+G(d) and MP2/6-31+G(d) computational results to predict four properties. The conclusions pertaining to these properties are as follows.

(1) The ring strain energy of the cage poly-yne decrease with every insertion of an ethynyl group. The ring strain energy of the ethynyl-expanded cubane **2** is only 32.5 kcal mol<sup>-1</sup> and the diethynyl-expanded cubane **18** and adamantane **20** are essentially strain-free. In addition, we note that B3LYP poorly predicts ring strain energy. However, a linear correction can be found so that the B3LYP results can closely mimic the MP2 values.

(2) The cyclic and cage poly-yne are very acidic, due to conjugation of the formal anionic center with the neighboring alkynyl groups. The most acidic compounds we examined are the diethynyl-expanded cubane **18** ( $\Delta G_{DPE} = 309.4$  kcal mol<sup>-1</sup>), prismane **14** ( $\Delta G_{DPE} = 309.2$  kcal mol<sup>-1</sup>), and tetrahedrane **5** ( $\Delta G_{DPE} = 312.6$  kcal mol<sup>-1</sup>). These are exceptionally low values for hydrocarbons.

(3) The poly-yne can serve as effective hosts for a lithium or sodium cation. The ideal host is one that can maximize the number of alkyne groups at the appropriate distance from the cation: C–Li distance of 2.3 Å and C–Na distance of 2.7 Å. The best host for Li<sup>+</sup> is **30**, while **33** and **2** are the best hosts for Na<sup>+</sup>.

(4) We utilized TDDFT/B3LYP/6-31+G(d) to evaluate the excitation energies of the poly-yne. While the method is insufficient to accurately reproduce the experimental values, relative trends can be discerned. The cyclic and cage poly-yne exhibit excitation energies significantly below that of the acyclic poly-yne. These lower excitation energies indicate that the alkynyl groups are interacting through space, even though isolated by an intervening saturated center. This interaction can extend into three directions, regardless of the angles between the alkynyl groups, as witnessed by the reduction in excitation values for all of the expanded tetrahedranes, prismanes, and cubanes. The same is true for the excitation energies of the conjugate bases of the poly-yne. Expanded adamantane, however, exhibits properties consistent with ordinary alkynes, showing no interaction between its alkynyl units.

Of all these properties, especially intriguing is the large variation in the excitation energies of the poly-yne, suggesting that molecules can be designed to have the specific absorption required for an optoelectrical device. We eagerly await the results of synthetic efforts to create these unusual molecules.

**Acknowledgment.** We are grateful for the financial support provided by the National Science Foundation and Trinity University for this research.

**Supporting Information Available:** The coordinates of all optimized structures at B3LYP/6-31+G(d) and MP2/6-31+G(d), their absolute energies, and the number of imaginary frequencies. This material is available free of charge via the Internet at <http://pubs.acs.org>.

JO060240I